

# Influence of the reaction conditions on the thermal stability of mesoporous MCM-48 silica obtained at room temperature

H.I. Meléndez-Ortiz\*, Y.A. Perera-Mercado, L.A. García-Cerda, J.A. Mercado-Silva, G. Castruita

*Centro de Investigación en Química Aplicada, Blvd. Enrique Reyna Hermosillo # 140, 25294 Saltillo, COAH, México*

Received 8 July 2013; received in revised form 15 August 2013; accepted 16 August 2013

Available online 26 August 2013

## Abstract

The thermal stability of MCM-48 silicas synthesized at room temperature under basic conditions using cetyltrimethylammonium bromide (CTAB) as template was evaluated as a function of the reaction time, CTAB/TEOS and H<sub>2</sub>O/ethanol molar ratios and ammonium hydroxide (NH<sub>4</sub>OH) concentration in the initial gel composition. Samples were characterized by X-ray diffraction (XRD), nitrogen adsorption–desorption analyses, scanning electron microscopy (SEM) and transmission electron microscopy (TEM). It was found that synthesis conditions affect the structural and thermal properties of the MCM-48 silicas. These silicas exhibited a size from 200 to 500 nm with spherical morphology.

© 2013 Elsevier Ltd and Techna Group S.r.l. All rights reserved.

**Keywords:** MCM-48 silica; Room temperature synthesis; Thermal stability

## 1. Introduction

The synthesis of a new family of mesoporous molecular sieves with regular and constant pore diameters from 2 to 10 nm, designated as M41S, was reported in 1992 by the scientists at Mobil Oil Corporation [1,2]. These mesoporous materials possess high specific pore volumes, high specific surface areas and narrow adjustable pore size distribution. Particularly, most of this research has been concentrated on MCM-41 silica because of its hexagonal arrangement of unidimensional mesopores with uniform and controllable pore diameter [3,4].

On the other hand, MCM-48 silica has been found to possess a bicontinuous structure centered on the gyroid minimal surface that divides available pore space into two nonintersecting subvolumes [5,6]. In comparison with MCM-41, the three dimensional pore structure of cubic MCM-48 seems more attractive for applications in adsorption, catalysis [7,8], chromatography [9], gas separation [10–12], and drug delivery [13,14] since it can avoid pore blockage [15,16]. Usually, mesoporous MCM-48 molecular sieves are synthesized by hydrothermal method in strong basic medium and their thermal stability has

been reported [17–19]. However, in 1999 Schumacher et al. [20] reported the synthesis of this silica at room temperature. Since then, many authors have reported the synthesis of MCM-48 at room temperature due to the advantages of this method, such as, short reaction times, power saving, and good reproducibility [21–23]. Nevertheless, thermal stability studies have not been carried out for these MCM-48 silicas synthesized at room temperature and using CTAB as template. The knowledge about this property is very important in catalysis, industrial applications, gas separation processes, etc.

Thus, the purpose of this work was to investigate systematically the effects of the synthesis time, CTAB/TEOS and H<sub>2</sub>O/ethanol molar ratios, and ammonium hydroxide concentration on the structural properties and thermal stability of the MCM-48 silicas prepared at room temperature. The obtained materials were characterized by X-ray diffraction, scanning electron microscopy, transmission electron microscopy and nitrogen adsorption–desorption isotherms.

## 2. Materials and methods

### 2.1. Materials

Tetraethyl orthosilicate, TEOS (98%, Aldrich) was used as the source of silica and cetyltrimethylammonium bromide, CTAB

\*Corresponding author. Tel.: +52 844 4389830x1335; fax: +52 844 4389839.

E-mail address: [ivan\\_melendez380@hotmail.com](mailto:ivan_melendez380@hotmail.com) (H.I. Meléndez-Ortiz).

(98%, Aldrich) as the structure directing agent. Deionized water obtained from a system of two ionic interchange columns, Cole-Parmer Instruments, ethanol (99.8%) and ammonium hydroxide,  $\text{NH}_4\text{OH}$  (29%) from Fermont were used to carry out the synthesis of mesoporous silica.

## 2.2. Preparation of mesoporous MCM-48 silica at room temperature

Synthesis of MCM-48 was carried out as follows: 2.6 g of CTAB was added to 120 mL of deionized  $\text{H}_2\text{O}$  and 50 mL of ethanol under stirring. When CTAB was completely dissolved, 12 mL of  $\text{NH}_4\text{OH}$  were added. After that, 3.6 mL of TEOS was poured into the solution immediately under vigorous stirring during 16 h at room temperature. The solid product was recovered by filtration and dried at room temperature overnight. The CTAB was removed from the inorganic material by calcining the sample at 540 °C for 9 h.

## 2.3. Thermal stability studies

In order to know the thermal stability of these materials, MCM-48 samples calcined at 540 °C were post-treated at different temperatures (650, 750 and 850 °C) by following calcination process. The heating rate was 2 °C/min and samples were kept during 6 h at the corresponding temperature.

## 3. Characterization

The powder XRD patterns were recorded on SIEMENS D5000 diffractometer using  $\text{CuK}\alpha$  radiation. The diffraction data were recorded in the  $2\theta$  range of 2–10°. The morphology of the samples was examined using a scanning electron microscope (JEOL JSM-7401F) operated at 5.0 kV. Transmission electron microscopy was performed using a HRTEM Titan operated at 300 kV.  $\text{N}_2$  adsorption–desorption isotherms were obtained using a Quantachrome AS1Win equipment at -196 °C. Before the experiments, the samples were degassed under vacuum at 250 °C for 10 h. The specific surface area of the sample was calculated using BET method. The pore size distribution was calculated using desorption branches of nitrogen isotherms and the density functional theory (DFT) method.

## 4. Results and discussion

In order to investigate the influence of various synthesis parameters on the formation and thermal stability of the MCM-48 materials, a series of reactions was conducted at room temperature by varying only one parameter at a time.

### 4.1. Influence of reaction time

Mesoporous MCM-48 silicas were prepared under magnetic stirring at different intervals of time from 1 to 16 h and their structural ordering was assessed by powder XRD. The XRD patterns of MCM-48 materials calcined at different temperatures are shown in Fig. 1. All the samples calcined at 540 °C

showed two major diffraction peaks, which correspond to the planes (211), (220), (420) and (332) that can be indexed to  $Ia3d$  cubic structure (Fig. 1(a)). Also, all MCM-48 silicas kept their cubic structure until a temperature of 750 °C (see Fig. 1 (b) and (c)). For all calcined samples, the  $d$ -spacing value for the plane (211) decreased as calcination temperature increased (see Table 1). However, samples synthesized at short reaction times (1, 4, and 8 h) showed the greatest decrease in this value. Their structure was destroyed by calcination post-treatment at 850 °C (Fig. 1(d)). This behavior indicates that these samples are less stable and collapse when temperature is raised. According to the literature, a longer stirring time is required to promote the silica condensation and it could prevent greater shrinkage of the mesostructure during calcination process [21]. On the other hand, samples synthesized at 14 and 16 h showed high-ordered structure at all temperatures and therefore, further analyses were carried out using a reaction time of 16 h. Additionally, the unit parameter cell (the center-to-center pore distance) ( $a_0$ ) was calculated by using  $d_{211}$ -spacing values according with the next equation [21]

$$a_0 = d_{211}(6)^{1/2} \quad (1)$$

From Table 2, it can be seen that the  $a_0$  values decreased when calcinations temperature increased. Newly, this shrinkage of  $a_0$  was more pronounced at short reaction times indicating that these samples are less stable to calcination post-treatment.

### 4.2. Influence of CTAB/TEOS molar ratio

The dependence of the CTAB concentration on thermal stability and structural order was also investigated. The CTAB/TEOS molar ratio in the initial gel was varied in the range of 0.15–0.3. The XRD diffractograms of MCM-48 silica obtained at different CTAB/TEOS molar ratios and calcined at 540 °C are shown in Fig. 2. Results showed that MCM-48 silica was not obtained when CTAB/TEOS molar ratio was 0.15. It means that an increase in the TEOS concentration results in silica materials with poor ordered structure due to an insufficient quantity of surfactant. In addition of a better stability in the entire mesostructure, the use of low CTAB/TEOS molar ratios could provide a framework thickness which is desirable for their use at high temperatures. By comparing XRD diffractograms of the silica samples synthesized at CTAB/TEOS molar ratio of 0.3 and 0.2, the first one had a better structural order due to the characteristic peaks of the plane (211) and (220) are more intense and sharper. Also, it can be seen from Table 2 that when CTAB/TEOS molar ratio decreased and post-treatment temperature increased, the lattice contraction of  $a_0$  was more pronounced (see samples 5, 6 and 7) indicating that the thermal stability, for the silicas prepared with low CTAB/TEOS molar ratio is reduced.

### 4.3. Influence of $\text{H}_2\text{O}$ /ethanol ratio

Since silicas prepared with a CTAB/TEOS molar ratio of 0.4 showed a better thermal stability, this molar ratio was chosen

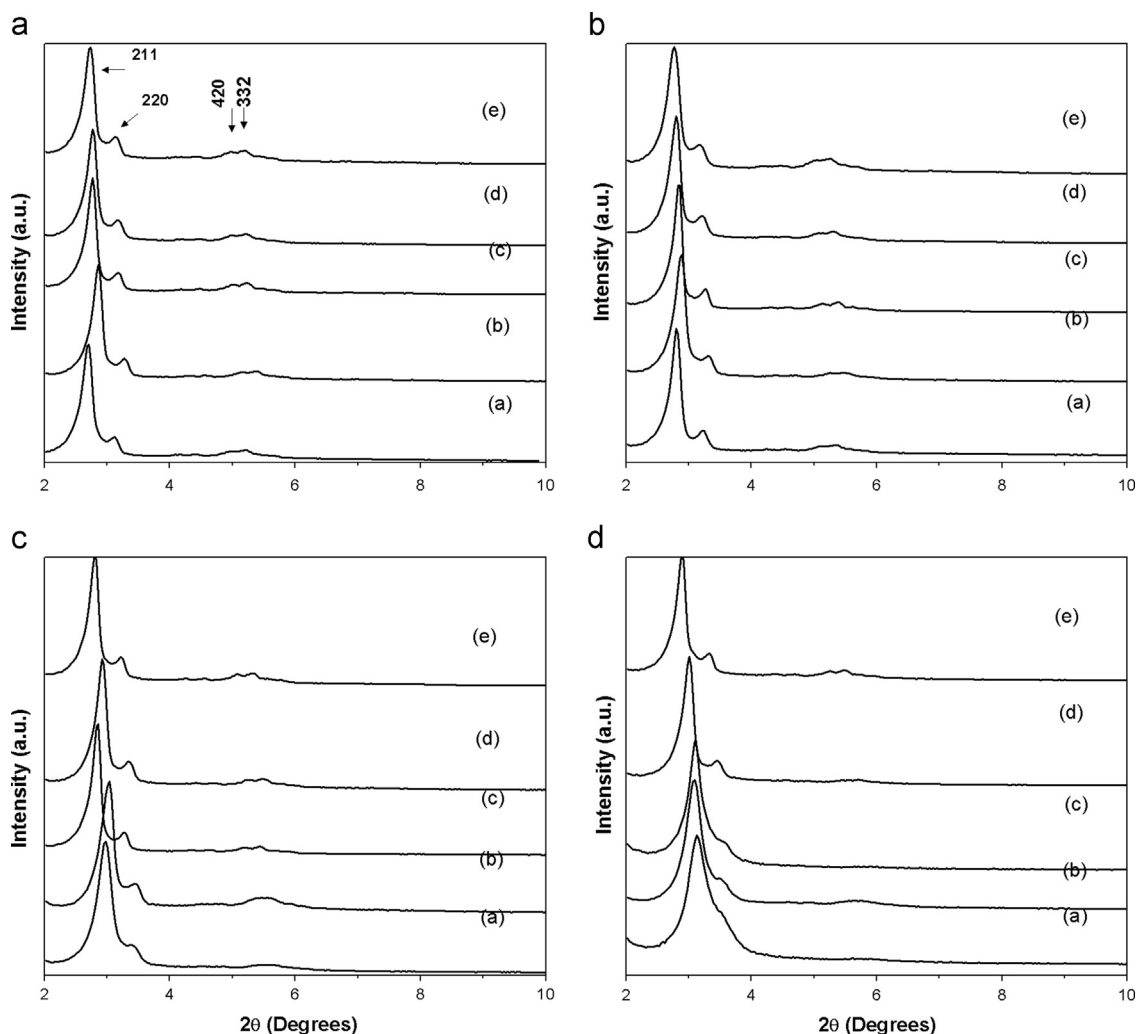


Fig. 1. Powder XRD patterns for MCM-48 samples synthesized at different reaction times: (a) 1 h, (b) 4 h, (c) 8 h, (d) 14 h and (e) 16 h. Calcination temperatures: (a) 540 °C, (b) 650 °C, (c) 750 °C and (d) 850 °C. CTAB/TEOS molar ratio of 0.4.

to carry out the next experiments varying H<sub>2</sub>O/ethanol molar ratio. It can be clearly seen from Fig. 3, that the formation of ordered MCM-48 depends strongly of H<sub>2</sub>O/ethanol molar ratio. If ethanol is added in low volume, MCM-48 structure is not formed. This is because the use of ethanol as co-surfactant increases the surfactant packing parameter and directs mesostructure assembly to a cubic MCM-48 [24]. On the other hand, we can observe that there is not a significant change in the unit cell parameter values by comparing samples 9 and 10 (Table 2) even when post-treatment temperature increases. This means that thermal stable MCM-48 silicas can be prepared using the range of H<sub>2</sub>O/ethanol molar ratio reported in this work.

#### 4.4. Dependence of NH<sub>4</sub>OH concentration

Since an optimum H<sub>2</sub>O/ethanol molar ratio range was found for the formation of MCM-48 silica at given CTAB/TEOS molar ratio, further synthesis trials were aimed at optimization of yet another gel compositional parameter, i.e. NH<sub>4</sub>OH concentration. For this purpose, different samples comprising a range from 0.3 to 0.15 mol of NH<sub>4</sub>OH were prepared and the quality and formation of MCM-

48 silica at room temperature were assessed. The powder XRD patterns of these samples post-treated at 850 °C are shown in Fig. 4. Sample synthesized with 0.15 mol of NH<sub>4</sub>OH exhibited only a broad peak at 2θ of 2.95 indicating that MCM-48 mesostructure was destroyed by effect of the post-treatment process while those samples prepared with 0.3 and 0.23 mol showed the presence of two clear reflections [(211), and (220)] indicating that MCM-48 structure is conserved after post-treatment. Also, the calculated cell parameter values for the silica synthesized with 0.15 mol decreased more significantly by comparing with silica samples prepared with 0.3 and 0.23 mol. This decrease indicates that the structure was contracted due to the increased condensation of silanol groups within the walls at high temperatures. Therefore, it can be concluded that, the concentration of NH<sub>4</sub>OH in the starting gel affects the thermal stability of MCM-48 silica synthesized at room temperature.

#### 4.5. Nitrogen adsorption–desorption studies

The nitrogen adsorption–desorption isotherms and pore size distribution of some MCM-48 silicas synthesized at different

Table 1

The d-spacing values of the plane (2 1 1) (nm) for MCM-48 silica synthesized at different parameters and post-treatment temperatures.

Sample	Reaction time (h)	d <sub>211</sub> -spacing value (nm)				
		As-synthesized	540 °C	650 °C	750 °C	850 °C
1	1	3.45	3.12	3.10	2.96	2.82
2	4	3.49	3.08	3.05	2.90	2.85
3	8	3.62	3.18	3.12	3.08	2.85
4	14	3.57	3.18	3.15	3.02	2.93
5	16	3.49	3.22	3.18	3.15	3.05
<b>CTAB/TEOS molar ratio</b>						
6	0.3	3.40	3.26	3.22	3.08	3.05
7	0.2	3.49	3.36	3.22	3.15	3.02
8	0.15	—	—	—	—	—
<b>H<sub>2</sub>O/ethanol molar ratio</b>						
9	7.7	3.49	3.22	3.18	3.15	3.05
10	9.0	3.62	3.22	3.18	3.18	3.08
11	11.1	—	—	—	—	—
<b>NH<sub>4</sub>OH moles</b>						
12	0.3	3.49	3.22	3.18	3.15	3.05
13	0.23	3.62	3.26	3.24	3.17	3.05
14	0.15	—	—	—	—	—

Table 2

The unit cell parameter values (nm) for MCM-48 silicas post-treated at different temperatures.

Sample	Reaction time (h)	Unit cell parameter, $a_0$ (nm)*				
		As-synthesized	540 °C	650 °C	750 °C	850 °C
1	1	8.45	7.64	7.59 (0.6%)	7.25 (5.1%)	6.91 (9.5%)
2	4	8.55	7.54	7.47 (0.9%)	7.10 (5.8%)	6.98 (7.4%)
3	8	8.87	7.79	7.64 (1.9%)	7.54 (3.2%)	6.98 (10.3%)
4	14	8.74	7.79	7.71 (1.0%)	7.40 (5.0%)	7.18 (7.8%)
5	16	8.55	7.89	7.79 (1.2%)	7.71 (2.2%)	7.47 (5.3%)
<b>CTAB/TEOS molar ratio</b>						
6	0.3	8.33	7.98	7.89 (1.1%)	7.54 (5.5%)	7.47 (6.3%)
7	0.2	8.55	8.23	7.89 (4.1%)	7.71 (6.3%)	7.40 (10.0%)
8	0.15	—	—	—	—	—
<b>H<sub>2</sub>O/ethanol molar ratio</b>						
9	7.7	8.55	7.89	7.79 (1.2%)	7.71 (2.2%)	7.47 (5.3%)
10	9.0	8.87	7.89	7.79 (1.2%)	7.79 (1.2%)	7.54 (4.4%)
11	11.1	—	—	—	—	—
<b>NH<sub>4</sub>OH moles</b>						
12	0.3	8.55	7.89	7.79 (1.2%)	7.71 (2.2%)	7.47 (5.3%)
13	0.23	8.87	7.98	7.93 (0.6%)	7.76 (2.7%)	7.47 (6.4%)
14	0.15	—	—	—	—	—

\*The values in parentheses correspond to the percentage of lattice contraction with respect to the MCM-48 silica calcined at 540 °C.

reaction conditions and post-treated at 850 °C are presented in Fig. 5a. Samples 5 and 6 showed nitrogen adsorption–desorption isotherms of type IV and a unimodal pore size distribution while sample 10 presented an isotherm of type I and a bimodal pore size

distribution. Also, it can be seen that samples 5 and 6 exhibited a steep condensation step in the relative pressure range of 0.2–0.3 which is associated with capillary condensation in the channels of MCM-48 [25,26]. The condensation was steep particularly for

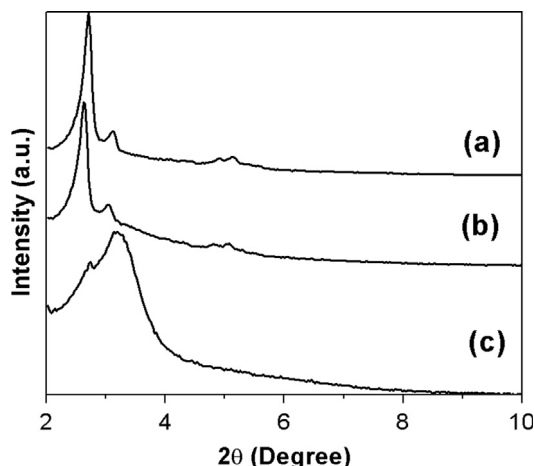


Fig. 2. XRD patterns of MCM-48 silicas calcined at 540 °C and synthesized at different CTAB/TEOS molar ratios: (a) 0.3, (b) 0.2, and (c) 0.15.

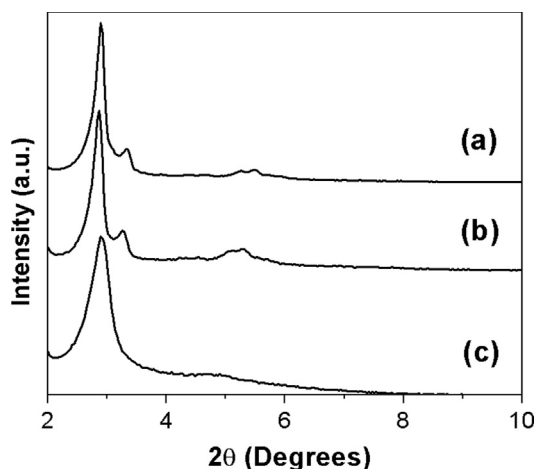


Fig. 3. Powder XRD diffractograms of MCM-48 samples prepared at different H<sub>2</sub>O/ethanol molar ratios: (a) 7.7, (b) 9 and (c) 11.1. Post-treatment temperature of 850 °C.

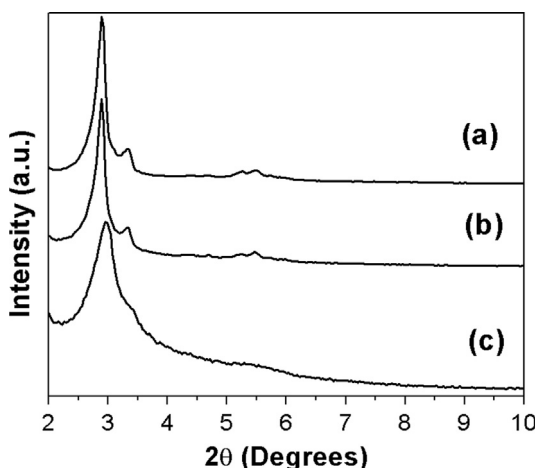


Fig. 4. XRD patterns of MCM-48 silicas calcined at 850 °C and synthesized at different NH<sub>4</sub>OH concentrations: (a) 0.3, (b) 0.23, and (c) 0.15 mol.

sample 5 indicating a good structural order by comparing with samples 6 and 10. These results are in agreement with those observed by XRD. However, all samples showed an average pore diameter under 2 nm (microporous region) (Fig. 5b). The specific pore volume, BET surface area, average pore diameter and estimated pore wall thickness deduced from the nitrogen sorption isotherms of various samples are summarized in Table 3. The wall thickness values were calculated by following Eq. (2) [27].

$$W_t = (a_0/3.092) - (\text{Pore diameter}/2) \quad (2)$$

High specific surface area values (higher than 1700 m<sup>2</sup>/g) were obtained for the sample 5 calcined from 540 °C to 750 °C. However, specific surface area, total pore volume and average pore diameter significantly decreased when calcination temperature was 850 °C. It means that at higher temperatures the pore structure collapses [22] and this could increase wall thickness [21]. Finally, the collapse was more evident for samples 6 and 10. It has been reported that the pore structure of MCM-48 silica prepared from TEOS completely collapses at temperature calcination of 750 °C [28]. However, the

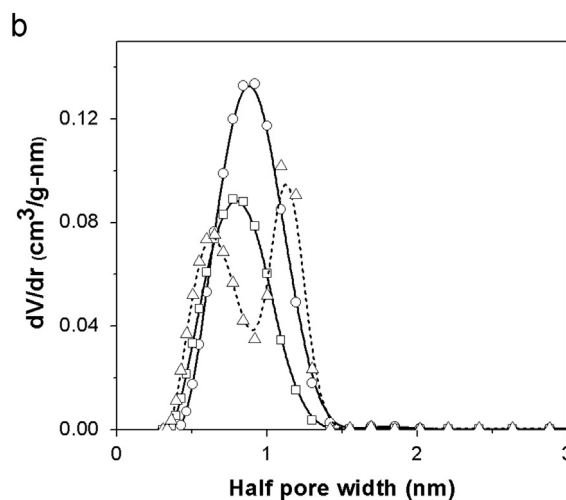
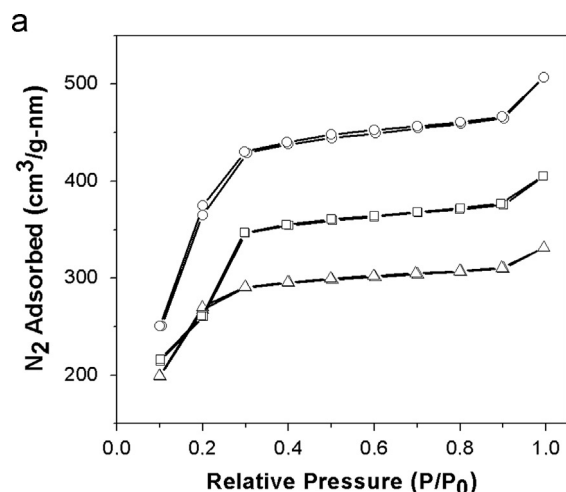


Fig. 5. Nitrogen adsorption–desorption isotherms (a) and pore size distribution (b) for MCM-48 synthesized at different reaction conditions: sample 5 (○), sample 6 (□) and sample 10 (△) and post-treated at 850 °C.



Table 3

Comparison of some structural parameters for MCM-48 samples obtained at room temperature under different reaction conditions.

Sample	Calcination temperature (°C)	Total pore volume (cm <sup>3</sup> /g)	BET surface area (m <sup>2</sup> /g)	DFT average pore diameter (nm)	Estimated wall thickness (nm)
5	540	0.824	1855	2.18	1.46
5	650	0.761	1700	2.18	1.43
5	750	0.799	1808	2.18	1.40
5	850	0.680	1494	1.83	1.50
6	850	0.451	935	1.54	1.64
10	850	0.549	1157	1.29	1.79

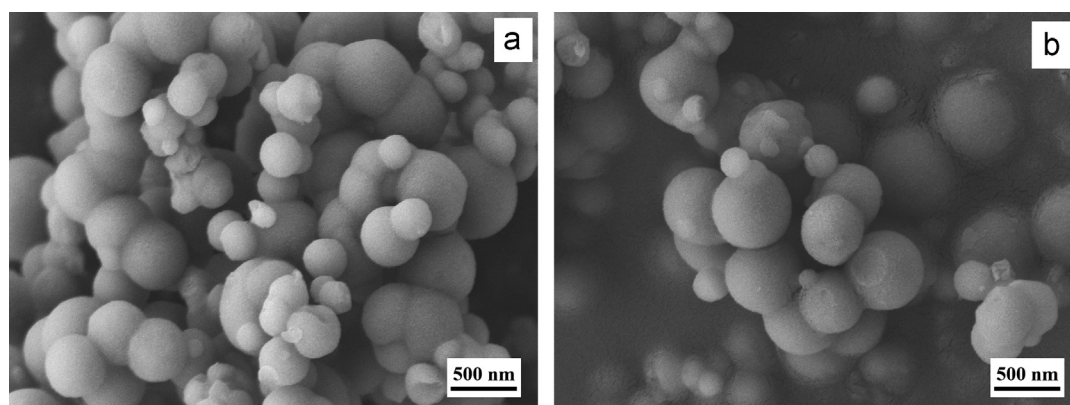


Fig. 6. Scanning electron micrographs of the MCM-48 (sample 5) calcined at (a) 540 °C and (b) post-treated at 850 °C. Synthesis conditions: reaction time of 16 h with a CTAB/TEOS molar ratio of 0.4.

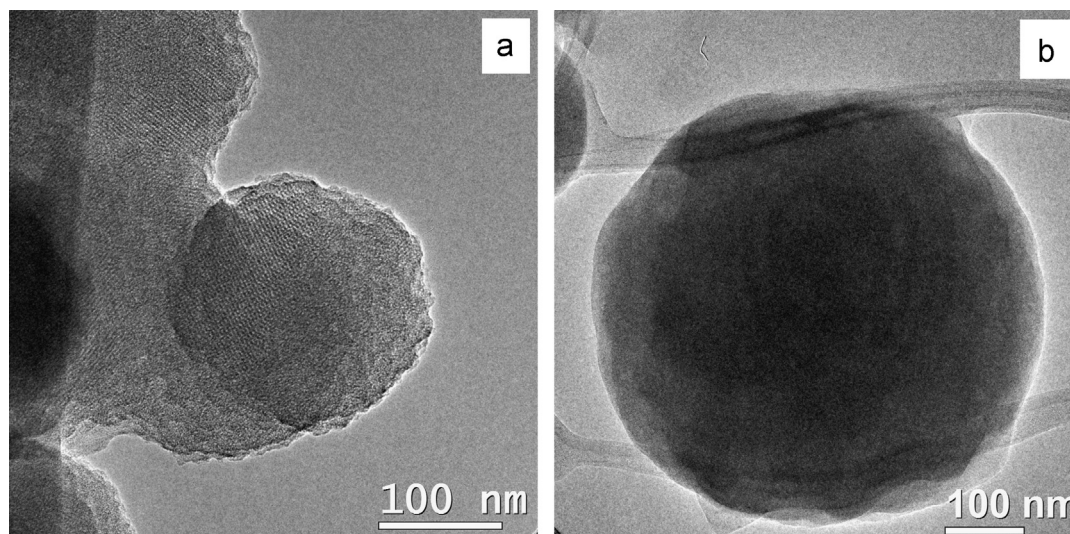


Fig. 7. Transmission electron micrographs of MCM-48 (sample 5) calcined at (a) 540 °C and (b) post-treated at 850 °C.

prepared MCM-48 at room temperature herein was very stable even under calcination at 750 °C during 6 h.

#### 4.6. Morphology studies

Scanning electron images of the mesoporous MCM-48 calcined at 540 °C and post-treated at 850 °C are shown in Fig. 6. It can be clearly observed that there are not morphological changes when

both silicas are compared. Both samples showed a spherical morphology with sizes from 200 to 500 nm. Further evidence for spherical morphology and pore structure is provided by the TEM images. Fig. 7a shows a TEM image of a MCM-48 particle calcined at 540 °C which showed a well-defined edge, a spherical shape and a regular pore structure over the whole particle. This spherical particle morphology may be due to the presence of ammonium hydroxide [15]. In the wide range, post-treated

MCM-48 sample (Fig. 7b) keeps its pore structural order in agreement with XRD results discussed in Section 4.1. However, N<sub>2</sub> adsorption–desorption studies showed that the pore size is reduced to microporous region when the sample is post-treated at 850 °C.

## 5. Conclusions

MCM-48 silicas have been prepared at different synthesis conditions and studied by XRD, SEM, TEM, and nitrogen adsorption–desorption studies. The structural properties and thermal stability of MCM-48 material can be tuned by varying reaction conditions such as synthesis time, molar ratios of CTAB/TEOS and H<sub>2</sub>O/ethanol in the initial gel composition. According to XRD and nitrogen adsorption–desorption analyses, high ordered mesostructure and thermally stable MCM-48 silica are obtained using CTAB/TEOS and H<sub>2</sub>O/ethanol molar ratios of 0.4 and 7.7 respectively. Also, a reaction time of 16 h is preferred to obtain silica nanoparticles with higher thermal stability. These mesoporous MCM-48 molecular sieves presented a uniform size and spherical morphology. The resulting size, shape uniformity and thermal stability until 750 °C of these MCM-48 silica particles should prove potentially useful for applications in catalysis, as catalyst supports, adsorbent and fillers in gas separation process as fillers membranes.

## Acknowledgments

This work was funded by the CONACYT – México (Fondo SENER-Hidrocarburos) under Grant no. 127499. The authors are grateful to J.A. Cepeda and E. Díaz for their technical assistance in the SEM and TEM studies respectively. Also, we thanks to H. Saade for the N<sub>2</sub> adsorption–desorption studies and B. Puente for technical assistance.

## References

- [1] C.T. Kresge, M.E. Leonowicz, W.J. Roth, J.C. Vartuli, J.S. Beck, Ordered mesoporous molecular sieves synthesized by a liquid-crystal template mechanism, *Nature* 359 (1992) 710–712.
- [2] J.S. Beck, J.C. Vartuli, W.J. Roth, M.E. Leonowicz, C.T. Kresge, K.D. Schmitt, C.T.W. Chu, D.H. Olson, E.W. Sheppard, S.B. McCullen, J.B. Higgins, J.L. Schlenker, A new family of mesoporous molecular sieves prepared with liquid crystal templates, *Journal of the American Chemical Society* 114 (1992) 10834–10843.
- [3] K. Moller, T. Bain, Inclusion chemistry in periodic mesoporous hosts, *Chemistry of Materials* 10 (1998) 2950–2963.
- [4] J.Y. Ying, C.P. Mehnert, M.S. Wong, Synthesis and applications of supramolecular-templated mesoporous materials, *Angewandte Chemie International Edition* 38 (1999) 56–77.
- [5] A. Monnier, F. Schüth, Q. Huo, D. Kumar, D. Margolese, R.S. Maxwell, G.D. Stucky, M. Krishnamurty, P. Petroff, A. Firouzi, M. Janicke, B.F. Chmelka, Cooperative formation of inorganic-organic interfaces in the synthesis of silicate mesostructures, *Science* 261 (1993) 1299–1303.
- [6] V. Alfredsson, M.W. Anderson, Structure of MCM-48 revealed by transmission electron microscopy, *Chemistry of Materials* 261 (1996) 1141–1146.
- [7] T. Jiang, D. Wu, J. Song, X. Zhou, Q. Zhao, M. Ji, H. Yin, Synthesis and characterization of mesoporous ZrMCM-48 molecular sieves with good thermal and hydrothermal stability, *Powder Technology* 207 (2011) 422–427.
- [8] Q. Dai, N. He, K. Weng, B. Lin, Z. Lu, C. Yuan, Enhanced photocatalytic activity of titanium dioxide supported on hexagonal mesoporous silica at lower coverage, *Journal of Inclusion Phenomena and Macrocyclic Chemistry* 35 (1999) 11–21.
- [9] V.M. Gunko, V.V. Turov, A.V. Turov, V.Z. Zarko, V.I. Garda, V. V. Yanishpolskii, I.S. Berezovska, V.A. Tertykh, Behaviour of pure water and water mixture with benzene or chloroform adsorbed onto ordered mesoporous silicas, *Central European Journal of Chemistry* 5 (2007) 420–454.
- [10] M. Bhagiyalakshmi, L.J. Yun, R. Anuradha, H.T. Jang, Synthesis of chloropropylamine grafted mesoporous MCM-41, MCM-48 and SBA-15 from rice husk ash: their application to CO<sub>2</sub> chemisorption, *Journal of Porous Materials* 17 (2010) 475–484.
- [11] H.Y. Huang, R.T. Yang, D. Chinn, C.L. Munson, Amine-grafted MCM-48 and silica xerogel as superior sorbents for acidic gas removal from natural gas, *Industrial and Engineering Chemistry Research* 42 (2003) 2427–2433.
- [12] S. Kim, J. Ida, V.V. Gulians, J.Y.S. Lin, Tailoring pore properties of MCM-48 silica for selective adsorption of CO<sub>2</sub>, *Journal of Physical Chemistry B* 109 (2005) 6287–6293.
- [13] I. Izquierdo-Barba, E. Sousa, J.C. Doadrio, A.L. Doadrio, J.P. Pariente, A. Martinez, F. Babonneau, M. Vallet-Regi, Influence of mesoporous structure type on the controlled delivery of drugs: release of ibuprofen from MCM-48, SBA-15 and functionalized SBA-15, *Journal of Sol–Gel Science and Technology* 50 (2009) 421–429.
- [14] A. Popat, J. Liu, Q.H. Hu, M. Kennedy, B. Peters, G.Q. Lu, S.Z. Qiao, Adsorption and release of biocides with mesoporous silica nanoparticles, *Nanoscale* 4 (2012) 970–975.
- [15] K. Schumacher, P.I. Ravikovitch, A. Du Chesne, A.V. Neimark, K. K. Unger, Characterization of MCM-48 materials, *Langmuir* 16 (2000) 4648–4654.
- [16] J. Xu, Z. Luan, H. He, W. Zhou, L. Kevan, A reliable synthesis of cubic mesoporous MCM-48 molecular sieve, *Chemistry of Materials* 10 (1998) 3690–3698.
- [17] L. Wang, J. Zhang, F. Chen, Synthesis of hydrothermally stable MCM-48 mesoporous molecular sieve at low cost of CTAB surfactant, *Microporous and Mesoporous Materials* 122 (2009) 229–233.
- [18] F.Y. Wei, Z.W. Liu, J. Lu, Z.T. Liu, Synthesis of mesoporous MCM-48 using fumed silica and mixed surfactants, *Microporous and Mesoporous Materials* 131 (2010) 224–229.
- [19] W. Zhao, Q. Li, Synthesis of nanosize MCM-48 with high thermal stability, *Chemistry of Materials* 15 (2003) 4160–4162.
- [20] K. Shumacher, M. Grün, K.K. Unger, Novel synthesis of spherical MCM-48, *Microporous and Mesoporous Materials* 27 (1999) 201–206.
- [21] T.W. Kim, P.W. Chung, V.S.Y. Lin, Facile synthesis of monodisperse spherical MCM-48 mesoporous silica nanoparticles with controlled particle size, *Chemistry of Materials* 22 (2010) 5093–5104.
- [22] K. Huo, L. Shen, F. Li, Z. Bian, C. Huang, Hemicyanine dye as a surfactant for the synthesis of bicontinuous cubic mesostructured silica, *Journal of Physical Chemistry B* 110 (2006) 9452–9460.
- [23] B. Boote, H. Subramanian, K.T. Ranjit, Rapid and facile synthesis of siliceous MCM-48 mesoporous materials, *Chemical Communications* 43 (2007) 4543–4545.
- [24] Y. Liu, A. Karkamkar, T.J. Pinnavaia, Redirecting the assembly of hexagonal MCM-41 into cubic MCM-48 from sodium silicate without the use of an organic structure modifier, *Chemical Communications* 37 (2001) 1822–1823.
- [25] W. Zhao, Z. Hao, C. Hu, Synthesis of MCM-48 with high thermal and hydro-thermal stability, *Materials Research Bulletin* 40 (2005) 1775–1780.
- [26] Y. Shao, L. Wang, J. Zhang, M. Anpo, Novel synthesis of high hydrothermal stability and long-range order MCM-48 with a conventional method, *Microporous and Mesoporous Materials* 86 (2005) 314–322.
- [27] K. Wang, Y. Lin, M.A. Morris, J.D. Holmes, Preparation of MCM-48 materials with enhanced hydrothermal stability, *Journal of Materials Chemistry* 16 (2006) 4051–4057.
- [28] K. Cassiers, T. Linssen, M. Mathieu, M. Benjelloun, K. Schrijnemakers, P. Van Der Voort, P. Cool, E.F. Vansant, A detailed study of thermal hydrothermal and mechanical stabilities of a wide range of surfactant assembled mesoporous silicas, *Chemistry of Materials* 14 (2002) 2317–2324.